

Analysis of Acoustic Wave from Supersonic Jets Impinging to an Inclined Flat Plate

S. Tsutsumi*, T. Nonomura, K. Fujii**, Y. Nakanishi***, K. Okamoto***, S. Teramoto****
Corresponding author: tsutsumi.seiji@jaxa.jp

* JAXA's Engineering Digital Innovation center, JAXA, Japan.

** Institute of Space and Astronautical Science, JAXA, Japan.

*** Department of Advanced Energy, University of Tokyo, Japan.

**** Department of Aeronautics and Astronautics, University of Tokyo, Japan.

Abstract: For the prediction and reduction of acoustic loading of launch vehicle at lift-off, acoustic wave radiated from ideally-expanded supersonic cold jets impinging to an 45-degree-inclined flat-plate, representative of a flame deflector, located 5D downstream from the nozzle exit is investigated numerically with the help of the experimental work. It turns out that dominant noise source is classified into three types: (i) the Mach wave radiation from free jet before the impingement, (ii) the acoustic wave generated from the impingement region, and (iii) another Mach wave radiation from supersonic wall jet after the impingement. Those features are clearly observed by applying the Proper Orthogonal Decomposition (POD) analysis to the numerical results. Comparing with the experimental result conducted in this study, prediction accuracy of 5 dB in OASPL is obtained in the current numerical simulation.

Keywords: Aeroacoustics, Launcher Acoustics, Large-Eddy Simulation.

1 Introduction

Propulsive power generated by the rocket engine is so significant that intense acoustic wave is radiated from the exhaust plume. Since the acoustic wave causes severe acoustic loading to the payload, prediction and reduction of the acoustic level around the launch vehicle at lift-off is quite important design issue taken into account early in the design process of the launch-pad. Several studies have been performed to understand and predict the launcher acoustics [1-4], but mechanism of acoustics radiated from rocket plume impinging to flame deflector is not evident yet. As such knowledge is essential to improve acoustic environment of launch vehicle, the present study aims to determine the noise generation from ideally-expanded cold jets impinging to a simplified flame deflector based on the Proper Orthogonal Decomposition (POD) analysis with Fourier transformation. Besides, verification and validation studies are conducted based on the experimental data taken in this study, and prediction accuracy of the present numerical method is assessed.

2 Problem Statement and Numerical Setup

Ideally-expanded cold jets with the exit Mach number of 1.8 and 2.0 are employed in this study. A flat plate inclined with 45 deg which is a simplified flame deflector is located 5D downstream from the nozzle exit. (D: nozzle exit diameter) The jet impinges to the inclined plate within the potential-core length. D is 20mm and the Reynolds number based on the nozzle exit is 1.64×10^6 in the experiment carried out at the University of Tokyo.

The computations are carried out with JAXA's in-house codes LANS3D, and UPACS-LES. The

governing equations of both of these two codes are three-dimensional compressible Navier-Stokes equations. The LANS3D is based on the finite differencing method using the overset structured grid. While, the UPACS-LES employs the finite volume method using the multi-block structured grid. The flowfield contains shock wave, but this study focuses on the aeroacoustics, so that higher-order method with shock-capturing capability is important. Therefore, for the LANS3D, modified seventh-order WCNS[5] is employed. While, for the UPACS-LES, 6th-order compact differencing scheme[6] with 10th-order low-pass filter.[7] In order to avoid non-physical oscillation at shock wave, the spatial derivatives at those regions are switched to the SLAU scheme[8] with the 2nd-order MUSCL interpolation. MILES approach[9] is adopted for the LANS3D, so any explicit LES sub-grid scale model is not used. Recently, this MILES approach using WCNS is also validated in basic turbulence flow.[10] While, the UPACS-LES employs the zonal LES/RANS hybrid method. The turbulent boundary-layer on the inclined plate is computed by the RANS with the Spalart-Allmaras model, and rest of the region is calculated by the LES with the standard SGS model. Both of the code employs implicit time integration. 2nd-order temporal accuracy is guaranteed by three-point backward differencing formula with Newton sub-iterations.

3 Mechanism of Acoustics based on POD Analysis

Numerical simulations of a M=2.0 ideally-expanded supersonic jet impinging on a flat-plate include with 45 degree were conducted based on the LANS3D.[11] Correlation between flow structure and acoustic field is discussed, and it turns out that, as shown in Fig.1, the acoustic wave is classified into three types;(i) the Mach wave radiation from the free jet before impingement, (ii) acoustic wave radiated from the impingement region, and (iii) another Mach waves radiation from supersonic wall jet. Considering the acoustic loading to a launch vehicle, the acoustic wave (ii) is important because it propagates directly upward to the vehicle. Since the flowfield contains oscillation of the plate shock, unsteady vortex shedding, and so on, it is difficult to distinguish the key feature leading to the acoustic wave (ii). Therefore, the POD analysis with Fourier transformation[12] is performed for better understanding of mechanism of acoustic wave (ii). As shown in Fig.2, time-series data of flowfield are transformed into several Fourier coefficients (complex value) with short time Fourier transformation. And then, the Fourier coefficients are used as a snapshot of POD analysis. After that, the complex value POD is conducted, and then, the most energetic modes are extracted. Owing to the POD analysis described here, most energetic modes for a limited frequency range can be extracted. Besides, each POD modes include information of phase information that is attractive for analyzing the noise source. Detail is given in the reference.[13]

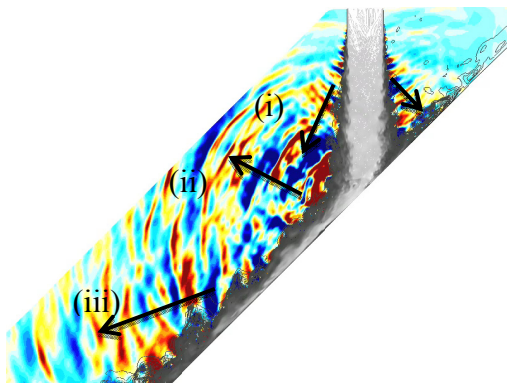


Fig.1 Acoustic field shown by the static pressure. Grey-colored contour line is the dynamic pressure.

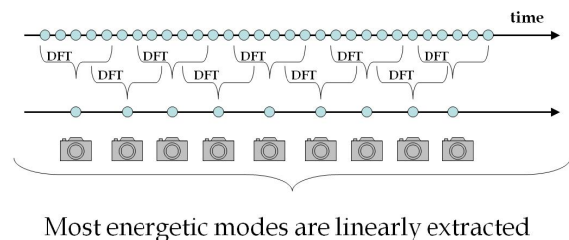
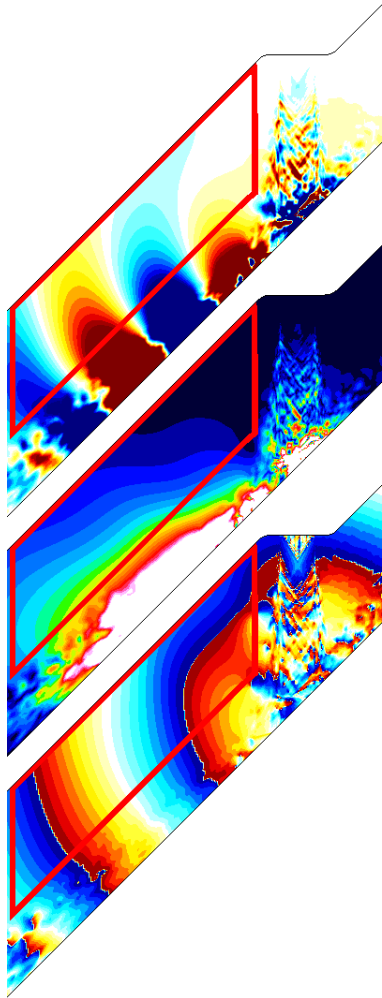
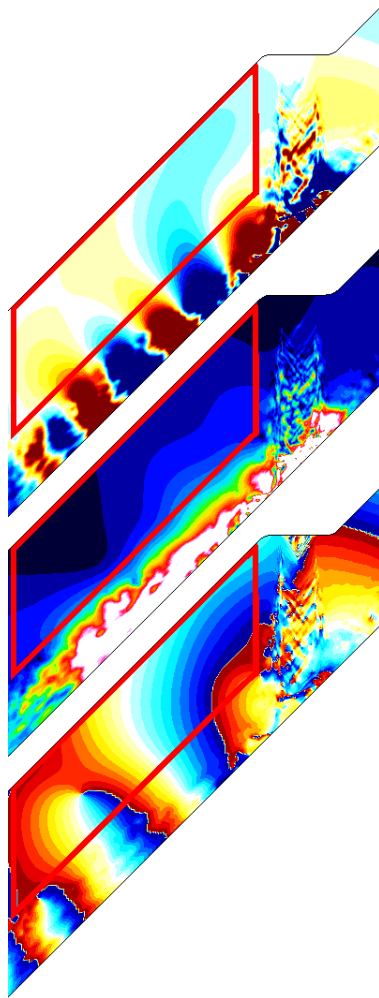


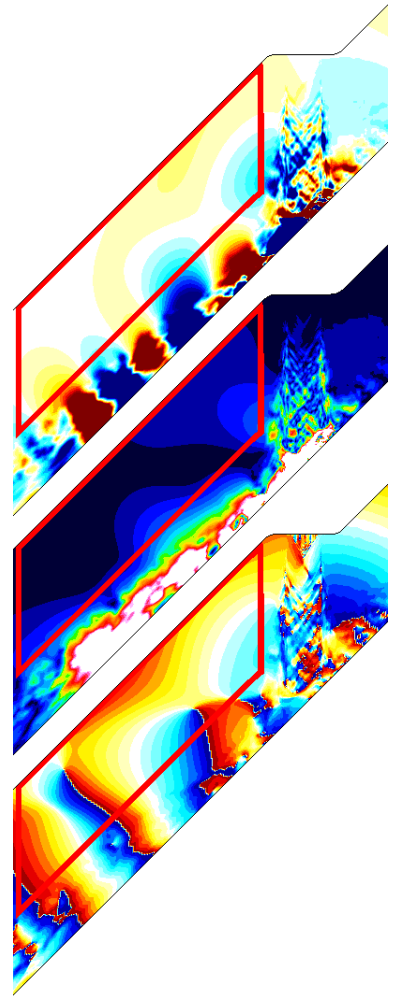
Fig.2 A schematic of snapshot POD with Fourier transformation.



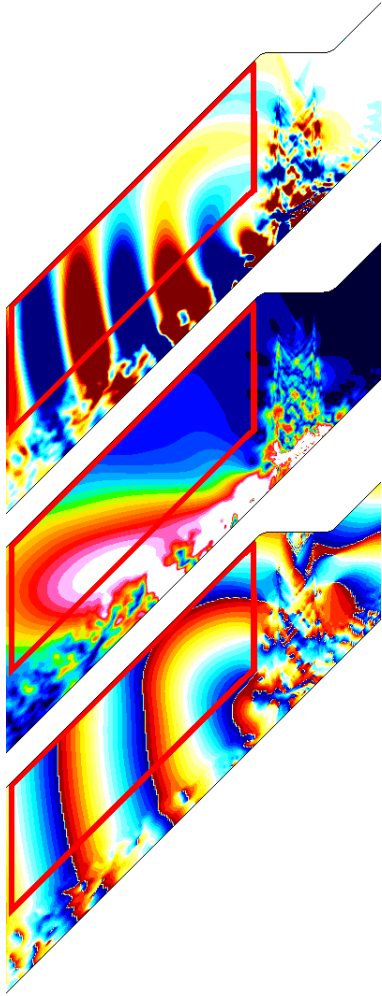
1st mode



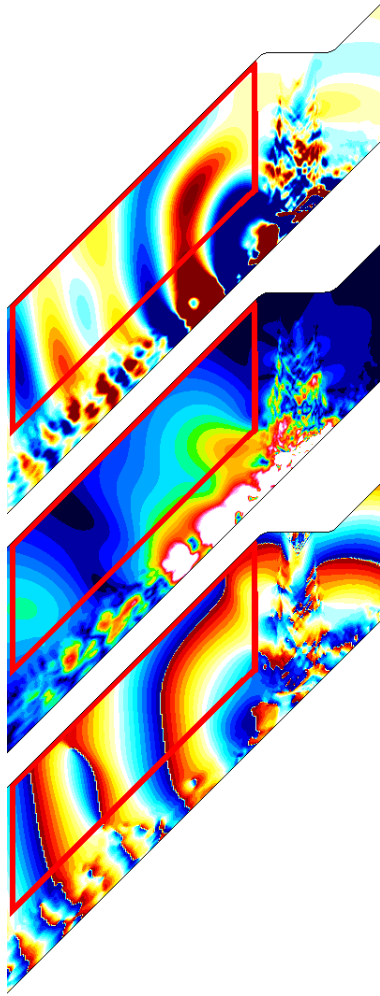
2nd mode
(a) $St=0.125$



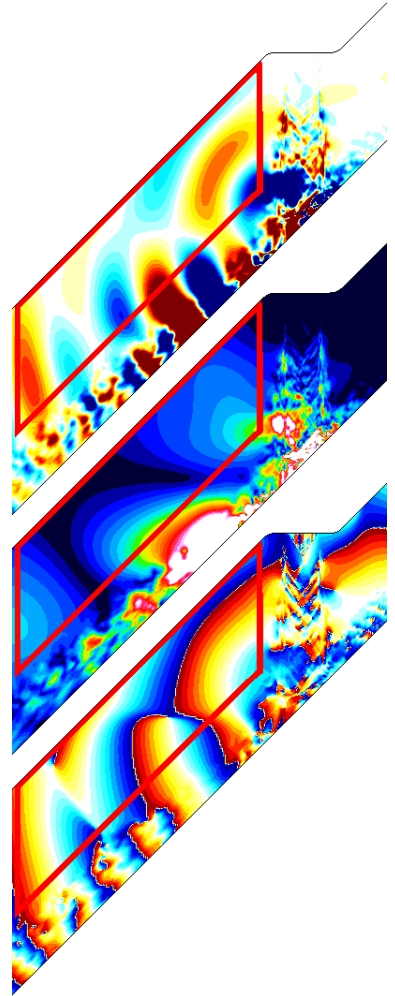
3rd mode



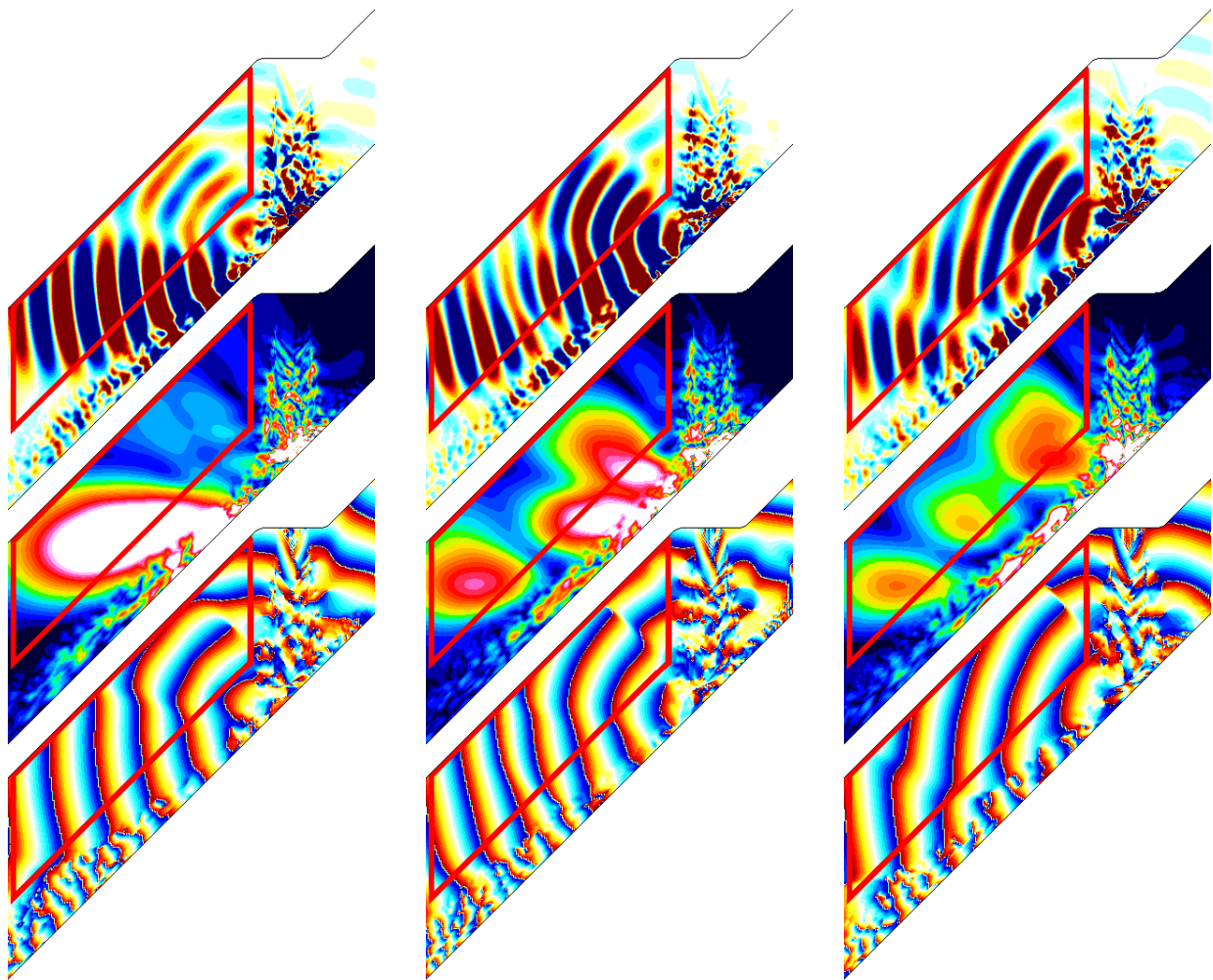
1st mode



2nd mode
(b) $St=0.25$



3rd mode

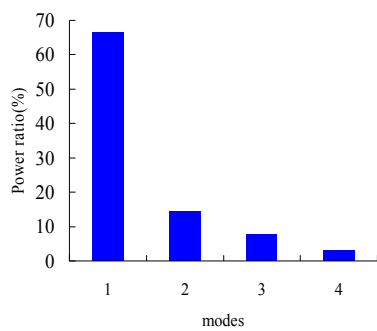


1st mode

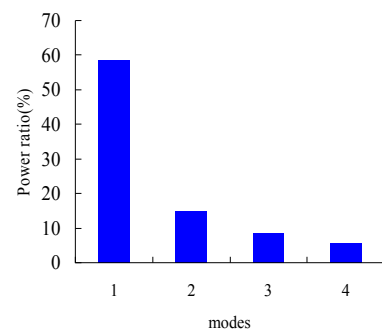
2nd mode
(c) $St=0.5$

3rd mode

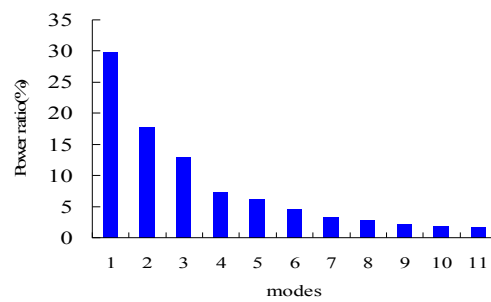
Fig.3 Result of POD. Top: real part, middle: magnitude, bottom: imaginary part.



(a) $St=0.125$.



(b) $St=0.25$.



(c) $St=0.5$.

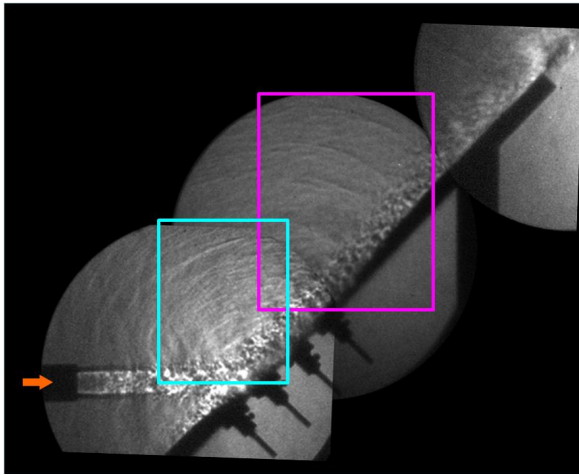
Fig.4 Power ratio of POD modes.

The POD analysis is conducted at three different Strouhal number: St, 0.125, 0.25 and 0.5. As shown in Fig.3, the POD analysis is applied to the two-dimensional pressure distribution that is bounded by the red lines. Energy ratio of each mode is shown in Fig.4. From this figure, it is found that 90% of the original flowfield is composed of first 4 modes at St=0.125 and 0.25. While for the result at St=0.5, 90% of the flowfield consists in 11 modes. In each figure of Fig.3, real part (top) magnitude (middle), and imaginary part (bottom) of the first 3 modes are shown. From the result of St=0.125 (Fig.3(a)), radiation of the Mach wave (iii) is observed in 1st mode. Other acoustic waves are not observed. From the observation of St=0.25 result, radiation of the Mach wave (iii) is more clear at 1st mode, and the acoustic wave (ii) starts to appear at 2nd and 3rd modes. At the highest frequency result in this study (St=0.5) displayed in Fig.3(c), the Mach wave (iii) is observed at all modes, while the acoustic wave (ii) is only observed in 2nd and 3rd modes. From the observation of the POD results, it is revealed that the Mach wave (iii) is a dominant noise source coming from the shear flow of the wall jet, but the Mach wave (iii) propagates obliquely downstream and causes little impact on the vehicle. On the other hand, the acoustic wave (ii) propagating directly to the vehicle is observed to be located where the plate shock interacts with the shear layer, and revealed to be the dominant noise source at high frequency range.

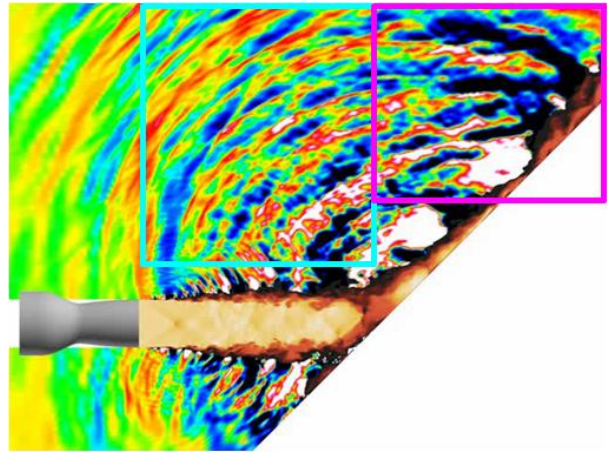
4 Prediction Accuracy of CFD

A supersonic nozzle designed to obtain M=1.8 at the nozzle exit is employed in the experiment. A flat plate inclined with 45 degree is located 5D downstream from the nozzle exit. The jet is exhausted in the ideally-expanded condition, and temperature ratio (=inflow total temperature/ambient temperature) is unity. The nozzle is carefully designed to obtain the exhaust flow parallel to the jet axis. Reynolds number based on the nozzle exit condition and the nozzle exit diameter (D=20mm) is 1.64×10^6 . The present experiment is carried out by using the hypersonic and high-temperature wind tunnel at the Kashiwa campus of the Tokyo University. Detail information is given in the reference.[14] Based on the experimental results, validation and verification of the UPACS-LES are conducted.

Experimental Schlieren image taken by the high-speed camera with 500 nsec exposure time is shown in Fig.5(a). Series of fine waves which propagates from the impingement region are observed at the cyan-colored region. Besides, distinct wave propagating obliquely downstream is observed at the magenta-colored region. Numerical result is shown by the static-pressure plot in Fig.5(b), and the same feature of the acoustic wave is observed. The series of the fine wave and the distinct wave observed here correspond to the acoustic wave (ii) and the Mach wave (iii), respectively. The OASPL at 40D far from the impingement point is compared with the measurements in Fig.6. Horizontal axis represents the angle from the jet axis. Three grid having different mesh size, 21M, 59M, and 120M, are compared here. Peak of the OASPL is observed at 75 degree from the jet axis in the experiment, while the peak appears at 80 deg in the numerical results. Among the numerical results, highest noise level is obtained by the 21M grid, while the result of the 120M grid shows lowest. Result of 59M grid is close to the 120M result where the angle is smaller than the 90 degree, but close to the 21M grid at higher angle. The 120M grid result is closest to the experiment among these three cases, but still overestimates the OASPL. Maximum difference of 5 dB is observed at 60 degree. The power spectrum density (PSD) is compared in Fig.7. Result obtained in the 120M grid is only displayed here. At $\theta=60$ degree, the numerical result overestimates. According to the result indicated in Fig.1, the Mach wave (iii) is a dominant noise source at the direction of $\theta=60$ degree. It is deduced that number of the grid point downstream from the impingement is not enough to resolve the shear layer of the wall jet. While, characteristics of the PSD agrees reasonably with the experiment at $\theta=90$ degree. At $\theta=135$ deg, present numerical result overestimates at low frequency region (St<0.6), but reasonable agreement is obtained at higher frequency region (St>0.6). As discussed here, key feature of the noise spectrum is reasonably obtained in the present numerical method.



(a) Schlieren Image (500nsec).



(b) Result of CFD. Acoustic wave is visualized by the static pressure, and jet flow by the Mach number.

Fig.5 Comparison of Near-field Wavefront.

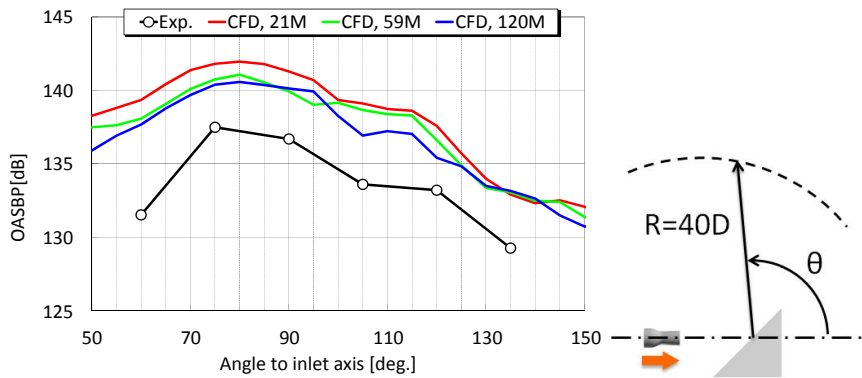
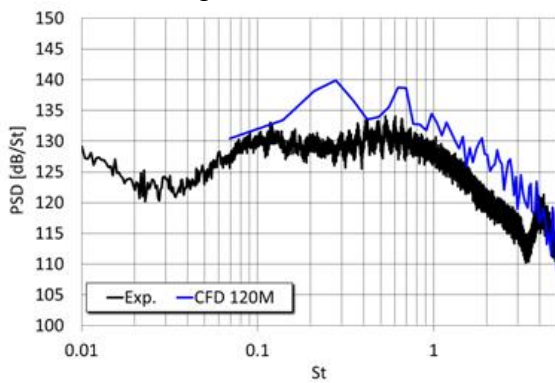
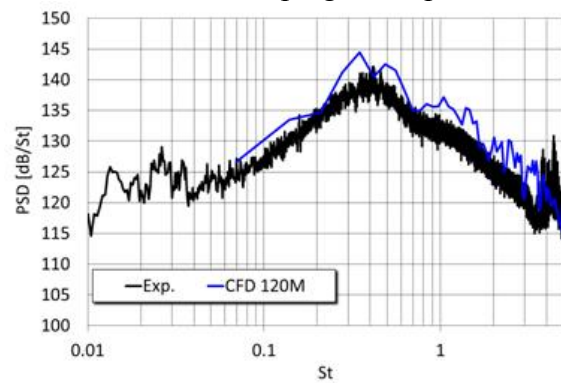


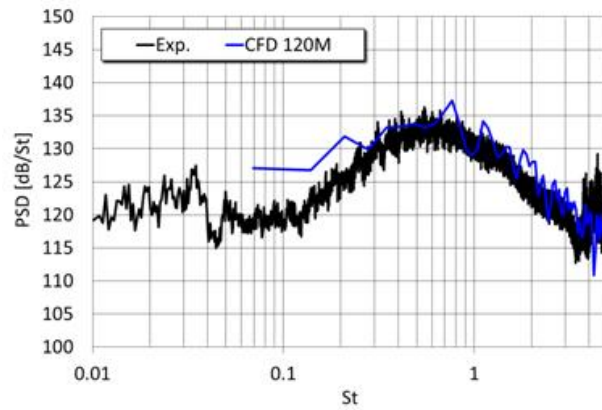
Fig.6 Comparison of OASPL distribution at 40D far from the impingement point.



(a) $\theta=60\text{deg.}$



(b) $\theta=90\text{deg.}$



(c) $\theta=120\text{deg}$.

Fig.7 Comparison of PSD spectrums at 40D far from the impingement point.

3 Summary

For the prediction and reduction of acoustic loading of launch vehicle at lift-off, numerical analysis is carried out to clarify mechanism of acoustic radiated from ideally-expanded supersonic cold jets impinging to a 45-degree-inclined flat-plate representing a flame deflector. The flat plate is located 5D downstream from the nozzle exit. Through the POD analysis with Fourier transformation, three types of acoustic waves are clearly extracted: (i) the Mach wave radiation from free jet before the impingement, (ii) the acoustic wave generated from around the impingement region, and (iii) another Mach wave radiation from supersonic wall jet downstream from the impingement. It is found that the Mach wave (iii) is a dominant noise source at all frequency range. While, the acoustic wave (ii) is the cause of the high frequency noise, and is generated where the plate shock interacts with the shear layer. In this study, validation and verification of the numerical method is also conducted based on the experimental results taken by the authors. Three grids having different mesh size are employed, and compared with the high-speed Schlieren image and microphone data at 40D far from the impingement point. The accuracy of prediction is confirmed to be 5dB in OASPL at the superfine grid case. PSD spectrum at each microphone is also compared, and it is found that key feature of noise spectrum is reasonably obtained in the present numerical method.

References

- [1] Eldred, et al., "Acoustic Loads Generated by the Propulsion System," NASA SP-8072, 1971.
- [2] Varnier, J., and Raguene, W., "Experimental Characterization of the Sound Power Radiated by Impinging Supersonic Jets," *AIAA Journal*, Vol. 40, No. 5, May 2002, pp. 825-831.
- [3] Koudriavtsev, V., Varnier, J., and Safronov, A., "A Simplified Model of Jet Aerodynamics and Acoustics," AIAA 2004-2877, May 2004.
- [4] Tsutsumi, S., Takaki, R., Shima, E., Fujii, K., and Arita, M. "Generation and Propagation of Pressure Waves from H-IIA Launch Vehicle at Lift-off," AIAA Paper 2008-390, 2008.
- [5] Nonomura, T., Goto, Y., and Fujii, K., "Improvements of efficiency in seventh-order weighted compact nonlinear scheme," Proceedings of 6th Asian Workshop on Computational Fluid Dynamics, AW6-16, 2010.
- [6] Kobayashi, M.H., "On a Class of Padé Finite Volume Methods", *Journal of Computational Physics*, Vol.156, pp.127-180, 1999.
- [7] Gaitonde, D.V., and Visbal, M.R., "Padé-Type Higher-Order Boundary Filters for the Navier-Stokes Equations", *AIAA Journal*, Vol.38, No.11, pp.2103-2112, 2000.
- [8] Shima, E., and Kitamura, K., "Parameter-Free Simple Low-Dissipation AUSM-Family Scheme for All Speeds," *AIAA Journal*, Vol.49, No.2, 2011, pp.584-590.
- [9] Boris, J. P., Grinstein, F. F., Oran, E., and Kolbe, R. J., "New Insights Into Large Eddy Simulation," *Fluid Dynamics Research*, Vol. 10, 1992, pp. 199-228.

- [10] Ishiko, K., Ohnishi, N., and Sawada, K., "Implicit LES of Compressible Turbulent Flow," AIAA 2007-920, 2007
- [11] Nonomura, T., Goto, Y. and Fujii, K., "Aeroacoustic waves generated from a supersonic jet impinging on an inclined flat plate," *International Journal of Aeroacoustics*, 2011, Vol.10(4), 401-426.
- [12] Suzuki, T., Bodony, D., Ryu, J., and Lele, S. K., "Noise Sources of High-Mach-number Jets at Low Frequencies Studied with a Phased-array Approach Based on LES Database," Annual research briefs 2007, Center for Turbulence Research, NASA Ames and Stanford University, 2007, <http://www.stanford.edu/group/ctr/ResBriefs/ARB07.html>.
- [13] Nonomura, T., Fujii, K., "POD of Aeroacoustic Fields of a Jet Impinging on an Inclined Plate," AIAA-2010-4019, June, 2010.
- [14] Nakanishi, Y., Okamoto, K., Teramoto, S., Okunuki, T., and Tsutsumi, S., "Acoustic Characteristics of Correctly-expanded Supersonic Jet Impinging on an Inclined Flat Plate", Asian Joint Conference on Propulsion and Power 2012, AJCPP2012-129, 2012.